Enhancing Image Quality of UDC Technology Through Novel Panel Design and Driving Method with MicroLED Display

Yu-Chieh Lin, Ying-Chieh Chen*, Chun-Liang Lin*, Chun-Han Tai*, Chun-Hsin Liu**
***Advanced Drive Development Div., AUO Corporation, Science Park, Hsinchu 300, Taiwan, R.O.C.**

Abstract
With the advancement of technology, integrating the display screen and front-facing lens into an under-display camera (UDC) device has become a breakthrough innovative technology for borderless and immersive visual experience. This article discusses the image quality improvement of micron light-emitting diode (Micro-LED) UDC technology and explains the relevant research results. Through time-sharing driver and pixel layout design optimization, the light spot problem is effectively solved, ensuring that the front screen can still display content normally when the UDC camera is shooting. In addition, through optical diffraction simulation and image quality analysis of different pixel designs, we successfully developed a low-diffraction pixel design suitable for Micro-LED UDC applications. Based on the above experimental results, we have successfully implemented Micro-LED UDC technology. This technology will be prioritized in the field of automotive display in the future, and we will continue to work on improving the quality of UDC images.

Author Keywords
Under-display camera (UDC); time sharing; sensor integration; Micro-LED; transparent display; automotive display.

1. Introduction
Under-display camera technology successfully integrates the display and photosensitive elements into a display device. This innovation eliminates the need for a visible front-facing camera module, allowing manufacturers to achieve larger, more immersive displays [1]. Compared with liquid-crystal display (LCD), Micro-LED and organic light-emitting diode (OLED) have self-luminous properties and do not require a backlight module, so they are more suitable for the development of UDC technology. In recent years, mainstream OLED mobile phones mainly use two design concepts to implement UDC [2], which are explained as follows:

Display quality considerations: The main feature of this technology is the consistent pixel per inch (PPI) between the main screen area and the UDC area. UDC has a better hiding effect; in order to improve the penetration rate, thin-film transistors (TFT) are placed outside the UDC area and the OLED device area within the UDC area is reduced. At the same time, transparent wiring (such as indium tin oxide) is used as a signal connection lines to significantly reduce the area of opaque metal in the UDC area.

Life time considerations: The main feature of this technology is to allocate more space to the penetration area and OLED devices without metal shielding by reducing the PPI of the UDC area; and integrating TFT and OLED on the same "island". The scanning and data signal lines between them are connected using metal. Therefore, the UDC area is clearly visible when the screen is lit.

Through the above two OLED UDC technical solutions, it can be clearly seen that the pixel design in the UDC area must strike a balance between the OLED devices size and PPI.

Compared with OLED, the advantage of Micro-LED is that it is an inorganic material and can withstand higher current density without affecting the lifetime due to reduction in devices size due to PPI or transmittance requirements. In addition, Micro-LED has the characteristics of high brightness, low power consumption and high reliability, so it is more suitable for transmissive display technology. However, as PPI increases, the impact of Micro-LED size on transmittance also increases, so shrinking Micro-LED size will become an important issue in the future.

However, when the display is placed in front of the camera, the display causes light to diffract, making the image blurry. Especially when strong light passes through the display, a flare phenomenon will occur [3]. At the same time, when the camera starts exposure, if the front monitor displays the image normally, it will also affect the image quality of UDC. In order to solve these problems, we have conducted in-depth research on the image quality improvement of Micro-LED UDC technology, focusing on the optimization of pixel design and driving methods.

2. UDC Image Quality Enhancement Method
In the current OLED UDC technology, it is well established that when the front camera is activated for photography, the OLED components in the UDC area are automatically turned off to prevent emitted light from impacting the UDC image, resulting in an appearance akin to a punch-hole display. Based on our research on Micro-LED UDC technology, we found that when the camera is operating and the UDC area displays content normally, there will be obvious light spots overlapping with the captured image, seriously affecting the image quality. Analysis found that the main reason for this abnormal phenomenon is that the light emitted by Micro-LED passes through the metal gaps, or the light is reflected by the interface of different materials in the cell and then captured by the camera. To ensure that the display in front of the UDC can function normally while maintaining the quality of the captured image, it is essential to effectively prevent the light emitted from the luminescent components from being captured by the camera. Therefore, to improve UDC image quality, the panel design focus is directed towards two main areas:

Backside light leakage improvement: The strategy is to use a metal layer to directly shield the light emitted by the Micro-LED towards the camera and reduce the reflected light caused by the difference in refractive index of each layer. Although this method may affect the transmittance, the impact of backlight leakage can be greatly reduced through reasonable design while meeting the transmittance requirements.

Drive timing optimization: The improvement of driving timing is achieved through time-sharing driving technology. The so-called time-sharing driving technology is to divide the light-emitting time of the Micro-LED display into several segments, that is, to adjust it to pulse light emission, so that the camera can complete the shooting within the interval time of emitting pulses. The light emission mode is adjusted to pulsed light emission, which causes the EM duty cycle to decrease, so the current density needs to be increased to maintain the same brightness. Due to the inorganic characteristics of Micro-LED, the instantaneous high current density during the emission process has a negligible impact on the characteristics and life of the components. In addition, in the drive setting, it is crucial to ensure synchronization and proper timing

ISSN 0097-996X/25/5602-1205-$1.00 © 2025

settings between the camera and the display, and the camera must have a global shutter function to obtain the best image quality.

Figure 1 illustrates the operation of time-sharing drive. Parameter A denotes the EM interval time, parameter B represents the time for one line, and parameter N indicates the time during which the camera cannot expose, equating to B multiplied by n, where parameter n relates to the camera's field of view (FOV) and the precision of the camera and display pairing. The Camera Exposure Time (CET) represents the maximum time the camera can expose, mathematically expressed as A minus N. In principle, CET can be set at any position within the A interval, depending on the configuration of the synchronous trigger signal between the display and camera. Setting CET at the front or rear yields the longest exposure time. In Figure 1, CET is positioned at the end of interval A. Theoretically, when the camera's exposure time is set to be less than or equal to CET, it can capture images normally without being influenced by light emitted from the Micro-LED.

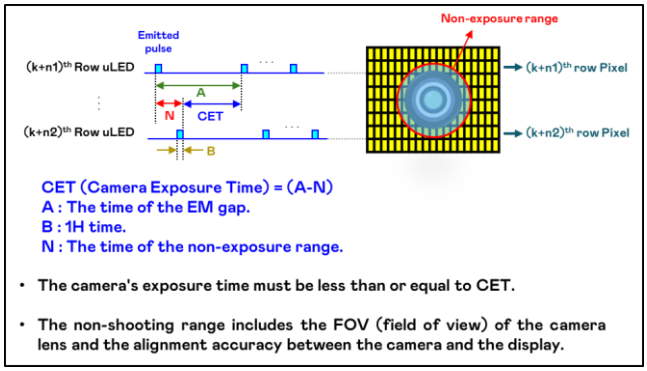

Figure 1. Description of time-sharing driving principle.

Figure 2 showcases the practical shooting results of the Time-sharing drive test utilizing a 13.5" FHD Micro-LED UDC display, where the UDC area displays audio-visual content normally during capture. Regarding the display timing setup, the number of EM pulses is set to 4, with A and N equating to 4166.67 (μs) and 2597.22 (μs) respectively, yielding a CET of 1569.44 (μs). To investigate the effects of different exposure times on image quality and light spots, the experiment set the exposure time range from 1.00 to 2.25 (ms) with an interval of 0.25 (ms), positioning CET at the front of interval A.

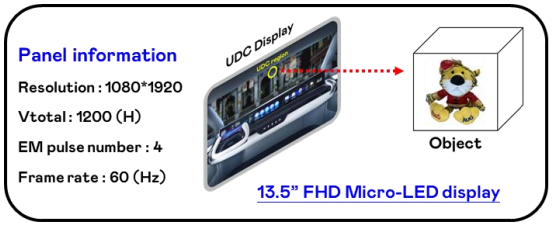

Timing setting	Value	Unit
Vtotal	1200	H
A	4166.67	μs
1H	13.89	μs
N	2597.22	μs
CET	1569.44	μs

Figure 2. Timing configuration for the time-sharing drive.

From the observations in Figure 3, when the exposure time is less than CET, it is evident that the captured image does not show micro LED light spots; regarding the darker image due to reduced exposure time, this can be optimized through image processing or adjustments to camera parameters. However, when the exposure time exceeds CET, light spots gradually appear, with light spots becoming visible above the UDC image when the exposure time is set to 1.75 (ms); at 2.25 (ms), the entire UDC image exhibits light spots.

Figure 3. Images quality using different exposure time settings.

The experimental results indicate that utilizing the pulsing emission characteristics of Micro-LED combined with time-sharing drive technology can realize a true full-screen display. Regardless of whether the under-display camera is currently capturing images, the UDC area can effectively display audio-visual content.

Another research focus aimed at improving UDC image quality pertains to pixel design. In order to address glare from strong light sources penetrating the display, we conducted optical diffraction simulations and image quality analyses on different pixel designs.

3. UDC Optical Diffraction Simulations and Image Quality Metrics

To deeply explore the interrelationship between UDC pixel design and diffraction optics, we established a set of optical diffraction simulation tools based on Fresnel diffraction theory. This will facilitate the analysis of the differences between simulated results and actual image quality. As shown in Figure 4(a), traditional

transparent pixel designs can typically be categorized into three regions: transparent area, component area, and interconnect area. In Micro-LED displays, considering the driving power consumption, TFT driving circuits are usually placed in the component area, which is also referred to as the "island." Adjacent islands are interconnected via metal interconnects. The geometric shapes of the interconnects and islands directly affect the optical properties of the transparent area.

To identify the most suitable pixel design for Micro-LED UDC displays, we studied four different pixel configurations. Figure 4(b) illustrates that conditions A and B feature rectangular islands, while conditions C and D feature circular islands. Conditions A and C incorporate rectangular metal interconnects, whereas conditions B and D utilize arc-shaped interconnects. All four configurations exhibit a pixel density of 100 PPI and a transmittance of 70%. Subsequently, we combined the optical diffraction simulation tools with image quality analysis methods for evaluation.

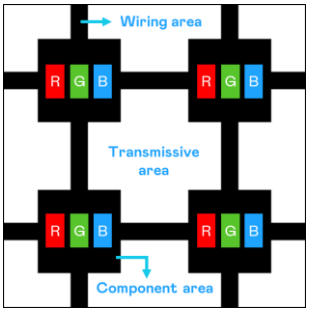

(a)

Design	A	B	C	D
Pixel Diagram (2*2)				
Island type	Square	Square	Circular	Circular
Trace type	Straight	Circular	Straight	Circular

(b)

Figure 4. (a) Micro-LED UDC pixel design diagram；(b) Pixel diagram of four different island and interconnect designs.

Optical diffraction simulation model: In optical diffraction theory, based on the definition of the Fresnel number, we can distinguish between Fraunhofer diffraction and Fresnel diffraction. The calculation of the Fresnel number is shown in Equation (1), where parameter A represents the aperture area, parameter D2 represents the distance between the aperture and the imaging system, and parameter λ denotes the wavelength received by the imaging system. When the Fresnel number exceeds 0.01, the light wave propagation occurs in the near field, which is categorized as Fresnel diffraction; conversely, when the Fresnel number is less than 0.01, it is referred to as Fraunhofer diffraction.

$$\text{Fresnel number} = \frac{A}{D2\times\lambda} \quad (1)$$

The optical diffraction model considers both Fresnel and Fraunhofer diffraction theories [4]. As illustrated in Figure 5, this model simulates a point light source passing through a transparent display and being captured by an imaging system (such as the human eye or a camera) as a point spread function (PSF). The model takes into account various factors such as object distance, observation distance, and the design of display pixels, alongside relevant parameters of the imaging system (e.g., aperture size and focal length). D1 represents the distance between the point light source or the observed scene and the transparent display; D2 indicates the distance between the display and the imaging system; A_{Iris} denotes the size of the camera aperture; and f stands for the camera focal length. When the light waves from the captured object pass through the transparent display and reach the camera aperture, the Fresnel number approaches 1. Therefore, the Fresnel diffraction formula is applied. When the light wave passes through the camera aperture and lens assembly, and is imaged on the CMOS sensor, the aperture size is significantly smaller than the focal length, so the Fraunhofer diffraction formula is utilized [5].

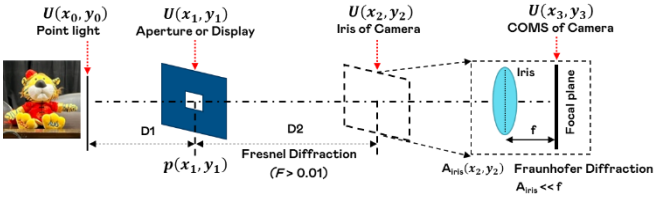

Figure 5. Fresnel diffraction simulation diagram.

We anticipate that the PSF in the simulation results will avoid forming distinct diffraction patterns, thereby preventing strong diffraction fringes from interfering with the system's ability to resolve images at specific locations. Therefore, in addition to observing the PSF patterns of different pixel designs, we also utilize the PSF to extract the Non-Diffraction Ratio (NDR) as one of the reference metrics for optical diffraction simulation. The physical significance of NDR lies in the proportion of light energy that passes through the transparent display without experiencing diffraction. As illustrated in the left part of Figure 6, the range of non-diffracted energy corresponds to imaging from the point light source through a completely transparent display. Parameter D represents its diameter, and E_0 is the total energy within diameter D; the numerical value of D is correlated with the settings of the imaging system. E_1 represents the total energy within diameter D after diffraction.

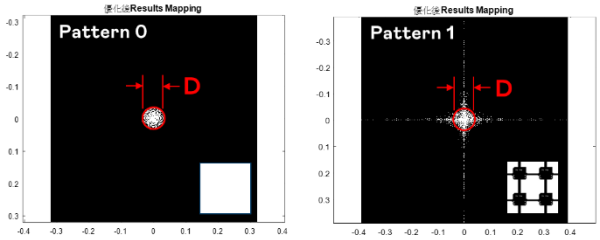

$$E_0 = \iint_D Power(x, y, Pattern\ 0)dxdy$$

$$E_1 = \iint_D Power(x, y, Pattern\ 1)dxdy$$

$$NDR = \frac{E_1}{E_0}$$

Figure 6. Definition of NDR.

Our findings indicate that a higher NDR value signifies that the energy following diffraction becomes more concentrated, enhancing image quality. Figure 6 defines the NDR (Non-Diffraction Ratio). Figure 7 presents the NDR, PSF, and the image of a red laser passing through the display for the aforementioned

four pixel designs. Overall, the design pattern in condition D exhibits the least diffraction results from the point light source, and energy is also the most converged. This indicates that the informational energy of the penetrated image is more concentrated and easier to recognize; conversely, condition A, with its fixed spatial frequency, leads to the most apparent diffraction effects. A comparative analysis of groups A and C with B and D shows that when the islands are rectangular, the diffraction effects are more pronounced. Thus, during design, the curvature variation of the islands is deemed more significant than that of the interconnects. The diffraction of light through the aperture area of the display primarily depends on the size of the aperture and its periodicity; the smaller the aperture and periodicity, the larger the diffraction angle. When the island is designed as a rectangle, the diagonal size of the aperture area is comparatively smaller than when the island is circular; thus, light easily generates larger diffraction angles. Furthermore, the periodicity of straight interconnects' aperture area is half that of arc-shaped interconnects, leading to larger diffraction angles for straight interconnects. Results show that the PSF and images of the red laser in conditions A, B, and C exhibit clear cross-shaped diffraction patterns due to the linear edges of the pixel designs. Condition A, particularly, where both the island and interconnects are linear, demonstrates the most significant diffraction impact and thus shows poorer visual performance and lower NDR values.

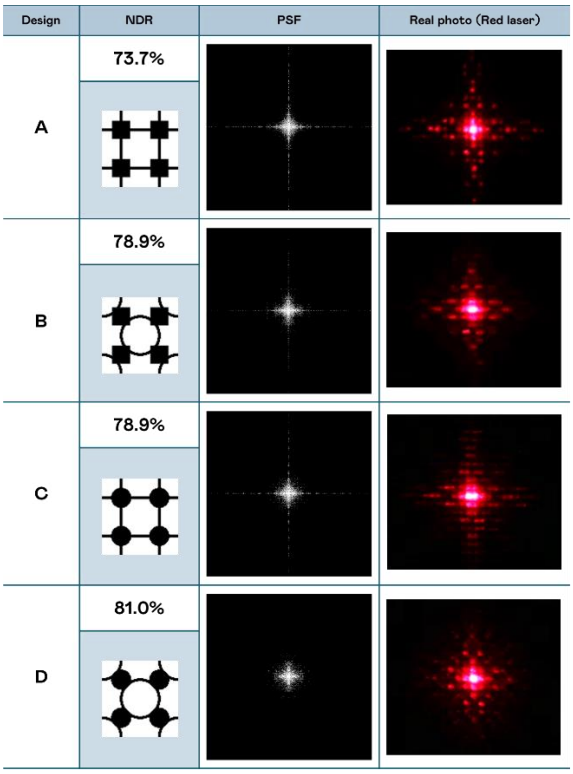

Figure 7. PSF simulation results and the diffraction pattern of red laser after passing through UDC pixels.

Image quality metrics: To further analyze the image quality of UDC displays, we established an optical measurement system specifically for UDC displays, used to capture images of different pixel designs. The evaluation of image quality considers the Structural Similarity Index (SSIM) [6, 7] and the Modulation Transfer Function (MTF). Figure 8 illustrates (a) NDR vs. SSIM and (b) NDR vs. MTF for different pixel designs. SSIM is used to compare the actual captured transmission image with a reference image that has not passed through the UDC display, and the object is an ISO12233 chart. The chart has patterns of different spatial frequencies, which is closer to the real environment. Of course, SSIM comparison can also be performed on specific spatial frequency patterns. MTF is the result of measuring a standard pattern with black and white slanted edges and calculating it using imatest tool. According to the evaluation results of different pixel designs displayed in Figure 8, the circular designs of islands and interconnects (condition D) exhibit the best diffraction characteristics, consistent with the trends shown in Figure 7. This validation method has also been applied to other pixel designs under varying PPI and transmittance, yielding similar results.

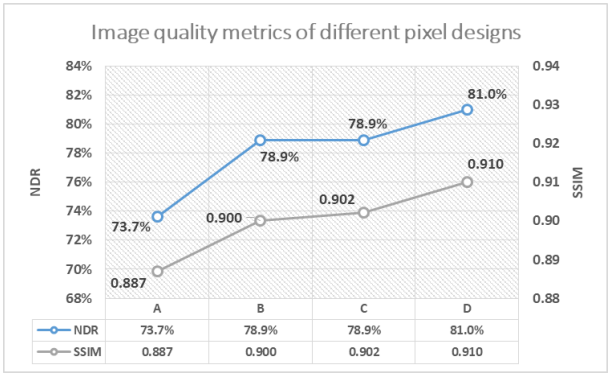

(a)

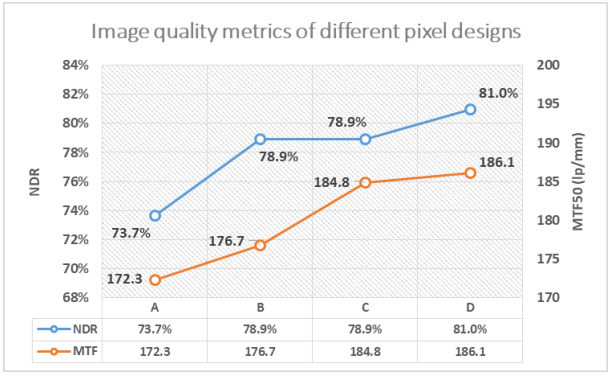

(b)

Figure 8. (a) Trends of NDR & SSIM；(b) Trends of NDR & MTF50.

Nevertheless, when both the islands and interconnects are designed as arcs, the impact on transmittance is quite significant. Therefore, regarding the pixel design for Micro LED transparent displays, we opted for arc-shaped interconnects, while ensuring the island edges undergo arc treatment, based on the requirement of satisfying product demand for transmittance, as displayed in Figure 9.

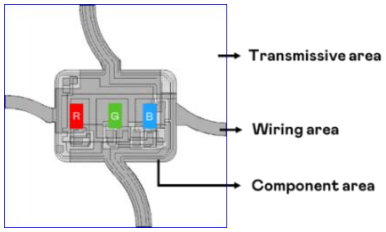

Figure 9. Pixel layout of Micro-LED UDC.(<100PPI).

4. Conclusion

In summary, based on the high brightness, reliability and pulse emission characteristics of Micro-LED, we have conducted a series of studies around Micro-LED UDC technology to deeply explore its future development potential, especially the improvement of UDC image quality. In order to enhance UDC image quality, we proposed a time-sharing drive method to ensure that the front monitor can display the image normally when the camera is exposed normally. In addition, in order to reduce the flare produced when a strong light source passes through the panel, our research targets optical diffraction simulation results of various pixel designs, such as PSF and NDR, as well as comparing actual captured images using SSIM and MTF analysis to determine the most suitable -Pixel design of Micro-LED UDC. We believe that the above efforts will greatly promote the future development of Micro-LED UDC technology in different application fields to achieve higher image quality.

5. References

1. Daewook Kim, Jaebum Cho, Jewon Yoo, Hyunjoo Hwang, Sungjae Park, Seungin Baek and Sungchan Cho, “Development of UDC Image Restoration Technology Using Space Variant CNN”, SID 2024 DIGEST • 735.
2. Benlian Wang, Yue Long, Hai Zheng, Ming Hu, Haijun Qiu, “A Novel OLED Full Display Technology with High Image Quality”, SID 2023 Symposium Digest of Technical Paper. Volume 54, Issue 1, 2023.
3. Rouf M, Mantiuk R, Heidrich W, Trentacoste M, Lau C. “Glare encoding of high dynamic range images” CVPR 2011. IEEE. 2011;289-296.
4. Bernard C. Kress, Patrick Meyrueis, “Digital Diffractive Optics: An Introduction to Planar Diffractive Optics and Related Technology”
5. Born and Wolf, “Principles of Optics”, p. 428
6. Zong Qin et al., IEEE Photonics Journal. Vol. 9, no. 4, August 2017.
7. Joseph W. Goodman , “Introduction to Fourier Optics”.